Theoretical Background: Hyperspectral Remote Sensing of Plant Functional Traits

Giorgi Kozhoridze

2025-10-24

Table of contents

1 Introduction: The Spectral Language of Vegetation

Remote sensing technology enables us to observe and quantify plant characteristics across scales, from individual leaves to entire ecosystems. At the heart of this capability lies the fundamental principle that different plant compounds interact uniquely with electromagnetic radiation (Gates et al. 1965). While human vision is limited to three broad spectral bands (red, green, and blue), hyperspectral sensors capture reflectance across hundreds of narrow, contiguous wavelength bands, revealing detailed information about plant biochemistry, physiology, and structure that remains invisible to the naked eye (Ustin and Gamon 2009).

The interaction between light and vegetation is governed by the absorption, transmission, and reflection properties of various biochemical compounds within plant tissues. Each pigment, structural component, and water molecule creates a characteristic spectral signature—a unique pattern of absorption and reflection across the electromagnetic spectrum (Jacquemoud and Baret 1990). By analyzing these signatures, we can non-destructively estimate pigment concentrations, assess physiological status, detect stress, and classify vegetation types (Peñuelas, Filella, Biel, Serrano, and Save 1993).

2 Seasonal Dynamics and Plant Functional Strategies

Plants exhibit remarkable temporal variability in their spectral properties, driven by phenological cycles, resource allocation strategies, and environmental responses (Richardson et al. 2018). Understanding these dynamics is fundamental to interpreting remote sensing data correctly.

Figure 1 illustrates the dramatic differences between plant functional types and their seasonal trajectories. The comparison between flowers/fruits and leaves demonstrates distinct spectral behaviors, while the seasonal progression from winter dormancy through spring leaf flush, summer maturity, and autumn senescence shows systematic changes in reflectance patterns (Huete et al. 2002). The tree diagrams depicting seasonal leaf development—from bare branches in winter, through flowering in spring, full canopy development in summer, to leaf senescence and abscission in autumn—provide a conceptual framework for understanding temporal spectral variability.

The distinction between mature leaves, juvenile leaves, and senescence leaves highlights that not all foliage within a canopy shares identical spectral properties (Asner and Martin 2015). This heterogeneity must be considered when scaling from leaf-level measurements to canopy or landscape observations.

Moreover, while the general phenological pattern—spring green-up, summer maturity, autumn senescence—is shared across many temperate plant species, the timing, magnitude, and spectral characteristics of these transitions vary systematically among species (Richardson et al. 2018; Asner and Martin 2015). Different species exhibit distinct phenological schedules: some leaf out earlier in spring, others maintain green foliage longer into autumn, and evergreen species

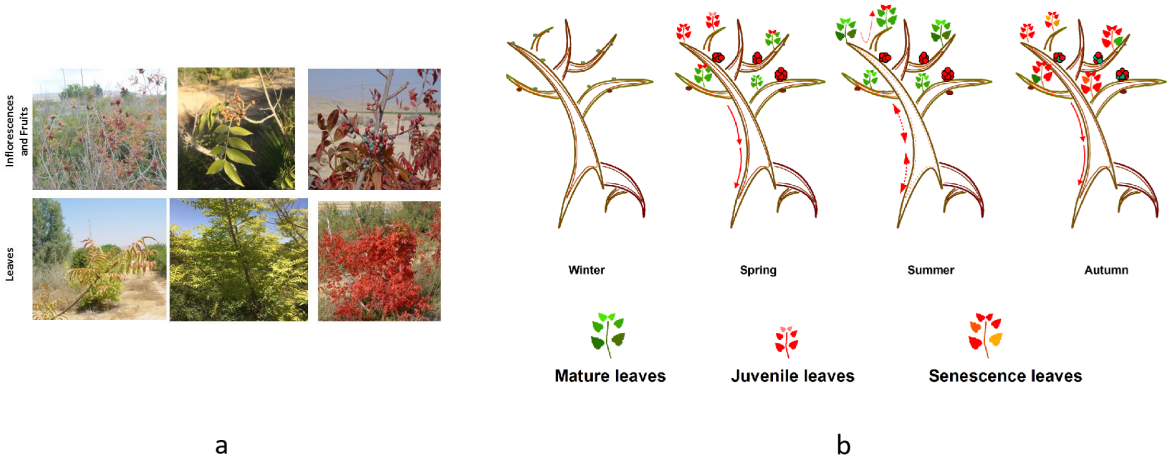

Figure 1: Seasonal phenological patterns in plant functional traits. a: Photographs showing inflorescence and fruits (top row) and leaf phenology (bottom row) in deciduous trees across seasons. b: Seasonal tree phenology diagrams from winter through autumn.

show entirely different seasonal patterns. These species-specific differences in phenological timing and pigment dynamics create unique spectral-temporal signatures that enable remote differentiation and mapping of plant species or functional types across landscapes (Ustin and Gamon 2009). By tracking how reflectance changes over time, rather than relying on snapshots from single dates, researchers can leverage these phenological differences to improve vegetation classification and monitor ecosystem composition (Hesketh and Sánchez-Azofeifa 2020).

3 Pigment-Specific Spectral Signatures

Pigment concentrations show typical temporal patterns throughout the growing season. Because each pigment type is characterized by specific spectral signature (Figure 2), specific concentrations of different pigments result in a specific overall spectral response of a leave. This enables us to detect phenology and health status of trees by spectral measurements. The following three key phenological stages can be determined:

1. **Early season dynamics** (March-May): Rapid increases in pigment concentrations as leaves develop, starting with anthocyanins (red juvenile leaves) and followed by chlorophyll content rising sharply during leaf expansion (Richardson et al. 2013).
2. **Mid-season stability** (June-August): Relatively stable biochemical composition during peak photosynthetic activity, though with notable variability reflecting environmental conditions and stress responses. Chloropylles are dominating (green mature leaves), unless stress conditions lead to increased dominance of other pigments (anthocyanins, carotenoids).

3. **Late season senescence** (September-October): Declining chlorophyll with differential changes in other compounds, creating the characteristic autumn coloration (Gitelson, Merzlyak, and Chivkunova 2001).

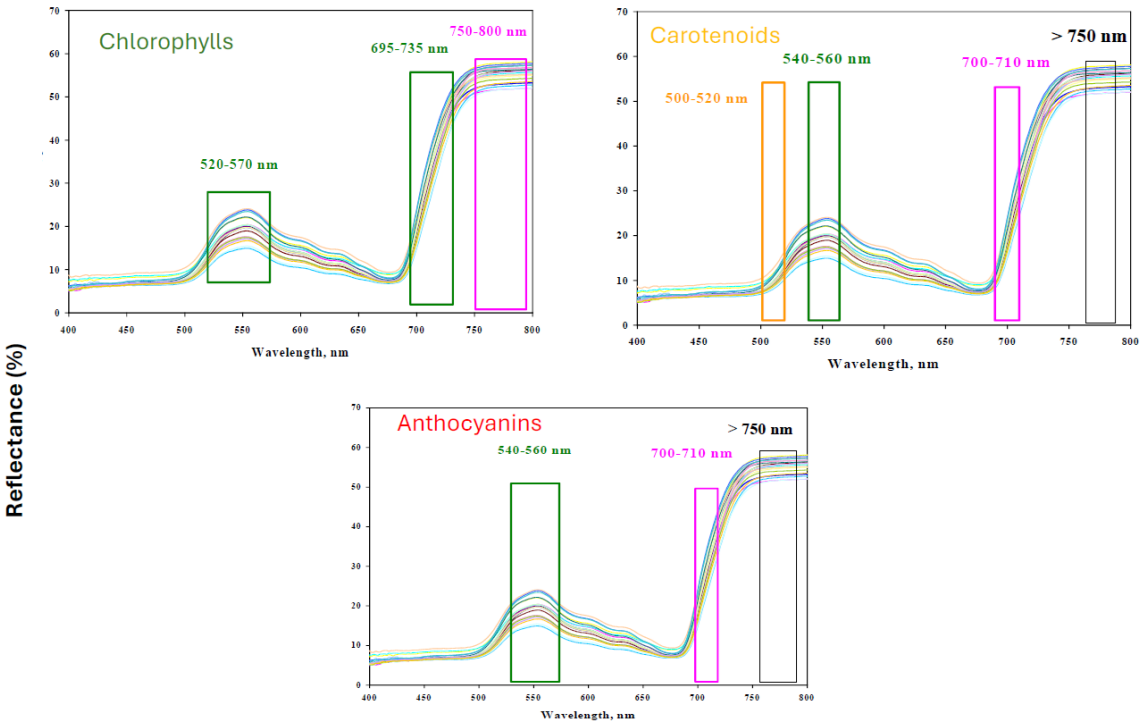

Figure 2: Spectral signatures of major plant pigments across the visible spectrum (400-800 nm). Top: Chlorophyll spectral reflectance showing characteristic absorption bands at 520-570 nm and 695-735 nm with near-infrared plateau at 750-800 nm. Middle: Carotenoid reflectance patterns with absorption features at 500-520 nm, 540-560 nm, and 700-710 nm. Bottom: Anthocyanin spectral signature showing strong absorption in the green-yellow region (540-560 nm) and at 700-710 nm. Colored boxes indicate key wavelength regions used in vegetation index formulations (Gitelson, Keydan, and Merzlyak 2006b).

3.1 Chlorophylls: The Primary Photosynthetic Pigments

Chlorophylls are the dominant pigments in healthy, photosynthetically active vegetation, and their spectral signature forms the foundation of vegetation remote sensing (Gitelson, Gritz, and Merzlyak 2003). Figure 2 shows the characteristic double absorption pattern of chlorophylls: strong absorption centered around 430 nm in the blue region and around 680 nm in the red region, corresponding to the absorption peaks of chlorophyll a and b (Lichtenthaler

1987). Between these absorption features, green light (520-570 nm) experiences relatively less absorption, explaining why healthy vegetation appears green to our eyes.

The key spectral regions for chlorophyll detection are:

- **Blue absorption** (430-490 nm): Primary absorption band, but less commonly used for chlorophyll estimation due to interference from carotenoids and atmospheric scattering (Gitelson et al. 2006)
- **Green peak** (520-570 nm): Local reflectance maximum where chlorophyll absorption is minimal
- **Red absorption** (660-690 nm): Deep absorption feature, highly sensitive to chlorophyll concentration
- **Red edge** (690-740 nm): Steep transition from red absorption to near-infrared plateau, extremely sensitive to chlorophyll content (Horler, Dockray, and Barber 1983)
- **Near-infrared plateau** (750-800 nm and beyond): High reflectance due to leaf internal structure, minimally affected by pigments (Gates et al. 1965)

The reciprocal reflectance model underlying vegetation indices for chlorophyll typically uses these wavelength regions (Gitelson, Keydan, and Merzlyak 2006a):

$$(1/R_{695-735} - 1/R_{750-800}) \times R_{750-800}$$

where the near-infrared term serves to normalize for structural effects and the difference in reciprocal reflectance quantifies chlorophyll absorption.

3.2 Carotenoids: Accessory Pigments and Photoprotection

Carotenoids serve dual roles in plant physiology: light harvesting in the photosynthetic apparatus and photoprotection against excess light energy (Demmig-Adams and Adams III 2006). Their spectral signature differs systematically from chlorophylls. Figure 2 demonstrates that carotenoids create characteristic absorption features in:

- **Blue region** (440-520 nm): Strong absorption overlapping with chlorophyll
- **Blue-green transition** (500-540 nm): Primary diagnostic region where carotenoid absorption distinguishes them from chlorophylls
- **Green region** (540-560 nm): Moderate absorption creating the yellow-orange appearance of carotenoid-rich tissues
- **Red region** (650-710 nm): Minimal absorption, contrasting with strong chlorophyll absorption

The spectral separation of carotenoids from chlorophylls becomes particularly important during senescence or stress conditions when the chlorophyll:carotenoid ratio changes dramatically (Gitelson et al. 2002). Vegetation indices designed to estimate carotenoids exploit the differential

absorption at 500-520 nm and 540-560 nm relative to the near-infrared reference, following a similar reciprocal reflectance formulation:

$$(1/R_{500-520} - 1/R_{700-710}) \times R_{750+}$$

3.3 Anthocyanins: Stress Response and Senescence Indicators

Anthocyanins represent a distinct class of pigments that accumulate in response to various stresses—environmental, pathogenic, or developmental (Gould 2004). Unlike chlorophylls and carotenoids, which reside in chloroplasts, anthocyanins accumulate in vacuoles and can mask the spectral signatures of photosynthetic pigments (Gitelson, Merzlyak, and Chivkunova 1999).

Figure 2 shows that anthocyanins create strong absorption in:

- **Green-yellow region** (540-600 nm): Primary absorption feature, explaining the red-purple appearance of anthocyanin-rich tissues
- **Overlap with chlorophyll green peak** (520-560 nm): This overlap complicates the interpretation of reflectance in this region

The reciprocal reflectance model for anthocyanins uses (Gitelson, Merzlyak, and Chivkunova 1999):

$$(1/R_{540-560} - 1/R_{700-710}) \times R_{750+}$$

where the denominator wavelength is chosen to minimize chlorophyll interference while capturing anthocyanin absorption.

The temporal dynamics of anthocyanin accumulation are particularly striking. Figure 3 displays spectral reflectance patterns across the growing season (March through October) with varying anthocyanin concentrations labeled on each panel. Key observations include:

1. **Spring accumulation** (March-April): Young, developing leaves often contain elevated anthocyanins (15-35 nmol/cm^2) for photoprotection during leaf expansion (Chalker-Scott 1999)
2. **Summer reduction** (May-August): Mature leaves typically maintain low anthocyanin levels (<7 nmol/cm^2) when plants are unstressed
3. **Autumn senescence** (September-October): Dramatic anthocyanin accumulation (up to 24 nmol/cm^2) as chlorophyll degrades and autumn coloration develops (Hoch, Zeldin, and McCown 2001)

The spectral manifestation of these changes is clearly visible in the green-yellow region (500-600 nm), where increasing anthocyanin content progressively suppresses reflectance. This seasonal pattern makes anthocyanin indices valuable for phenological monitoring and stress detection (Gitelson et al. 2006).

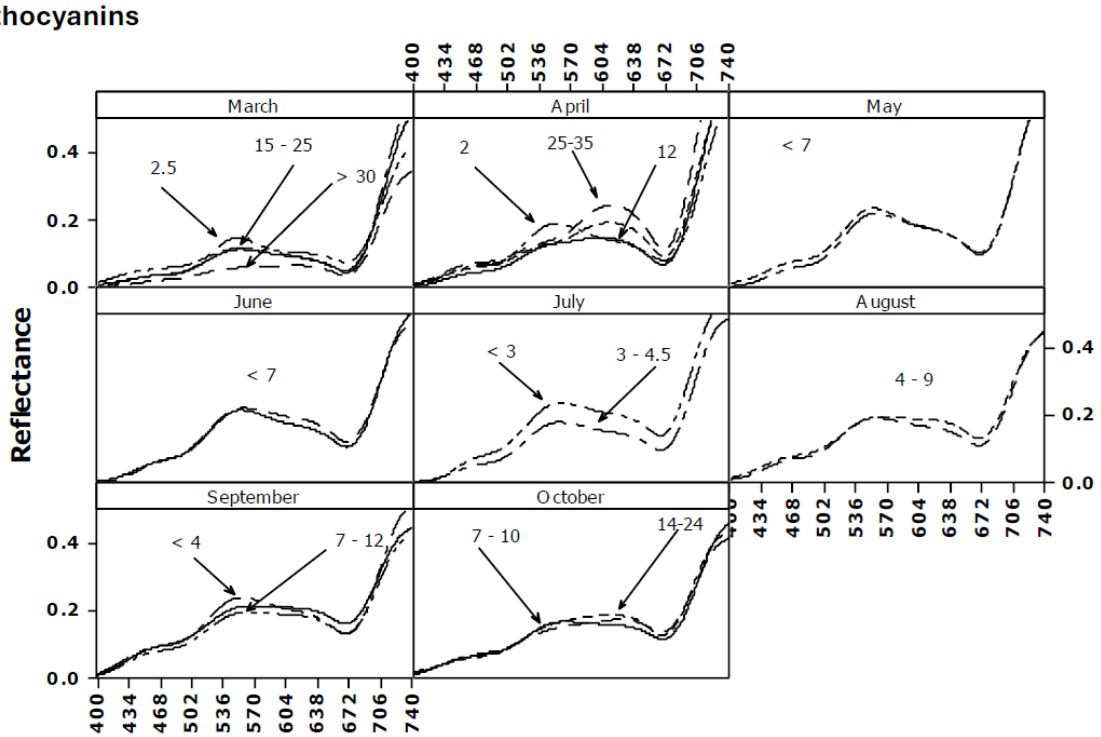

Figure 3: Seasonal variation in anthocyanin content and spectral reflectance. Spectral reflectance curves from March through October showing changes in reflectance patterns (400-750 nm) associated with varying anthocyanin concentrations (labeled in nmol/cm^2). Spring months (March-April) show elevated anthocyanin in developing leaves, summer months (May-August) display minimal anthocyanin in mature leaves, and autumn months (September-October) exhibit dramatic anthocyanin accumulation during senescence. The green-yellow region (500-650 nm) shows progressive absorption with increasing anthocyanin content.

4 Concentration-Dependent Spectral Response

The relationship between biochemical concentration and spectral reflectance follows predictable patterns that enable quantitative remote sensing (Jacquemoud and Baret 1990). Figure 4 provides a comprehensive demonstration of this relationship for chlorophylls and carotenoids.

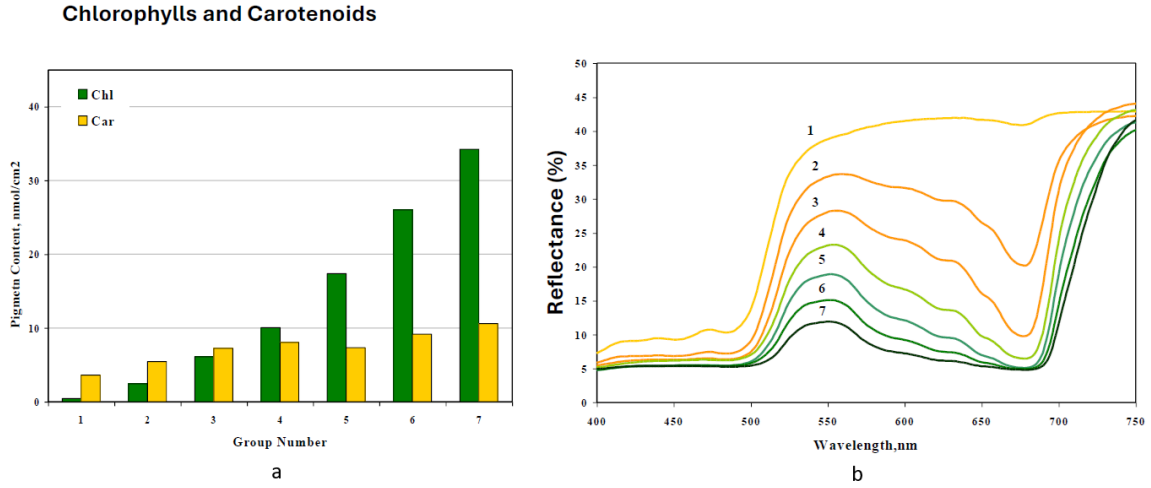

Figure 4: Concentration-dependent spectral response of chlorophylls and carotenoids. a: Pigment content (nmol/cm²) for chlorophyll (Chl, green bars) and carotenoids (Car, yellow bars) across seven groups with increasing chlorophyll dominance. b: Corresponding spectral reflectance curves (400-750 nm) for each concentration group, showing systematic changes in reflectance magnitude and spectral shape.

The left panel of Figure 4 shows chlorophyll (Chl, green bars) and carotenoid (Car, yellow bars) concentrations across seven groups with increasing biochemical content and chlorophyll dominance. Group 7 contains approximately 35 nmol/cm² of chlorophyll and 10 nmol/cm² of carotenoids, representing dense, healthy foliage, while Group 1 has minimal pigment content dominated by carotenoids, which is characteristic of stressed or senescent tissue.

The right panel shows how these concentration differences manifest in spectral reflectance (400-750 nm). The numbered curves (1-7) correspond to the concentration groups, revealing several critical patterns:

1. **Blue region** (400-500 nm): All curves show low reflectance due to combined chlorophyll and carotenoid absorption, with minimal differentiation between concentration levels.
2. **Green peak** (520-570 nm): Increasing pigment concentrations progressively suppress the green reflectance peak, but this region shows modest dynamic range.
3. **Red absorption** (650-690 nm): Deep absorption trough that deepens only slightly with increasing chlorophyll concentration due to saturation effects.

4. **Red edge** (690-750 nm): The most dramatic differentiation occurs here, where the slope and position of the red edge shift systematically with chlorophyll content (Horler, Dockray, and Barber 1983).

Note the near-linear spacing of curves as pigment concentration increases in the red edge region. This high sensitivity in the red edge makes it the most valuable spectral region for chlorophyll estimation (Gitelson, Keydan, and Merzlyak 2006a). The physical explanation involves the transition from strong chlorophyll absorption in the red to minimal absorption in the near-infrared, creating a steep gradient that shifts in both position (red edge position) and amplitude with changing chlorophyll content.

This concentration-reflectance relationship forms the empirical foundation for vegetation indices and regression-based retrieval algorithms (Verrelst et al. 2015). However, the relationships are not always linear due to:

- **Saturation effects**: At high pigment concentrations, absorption becomes nearly complete, reducing sensitivity (Gitelson, Gritz, and Merzlyak 2003).
- **Multiple scattering**: Photon path length through leaf tissue affects the absorption probability.
- **Package effects**: Pigments organized in chloroplasts rather than uniformly distributed. (Jacquemoud and Baret 1990)
- **Structural confounding**: Leaf thickness, internal air spaces, and surface properties modulate reflectance independently of biochemistry (Asner 1998).

5 Phenological Stages and Stress Detection

As we stated above, the appearance of foliage across developmental stages and stress conditions creates distinct spectral signatures that enable phenological monitoring and early stress detection (Carter 1993). Figure 5 presents a comprehensive comparison of three critical vegetation states: green (healthy) leaves, yellow-reddish (stress/senescence) leaves, and red (early development) leaves.

5.1 Green Leaves: The Baseline Healthy Signature

The green leaf spectra (top left, Figure 5) exhibit the classic vegetation signature (Gates et al. 1965):

- Low reflectance in blue (400-500 nm) and red (600-680 nm) due to chlorophyll absorption
- Modest green peak around 550 nm where chlorophyll absorption is minimal
- Sharp red edge transition (690-750 nm)
- High near-infrared plateau (750-800 nm) determined by leaf internal structure

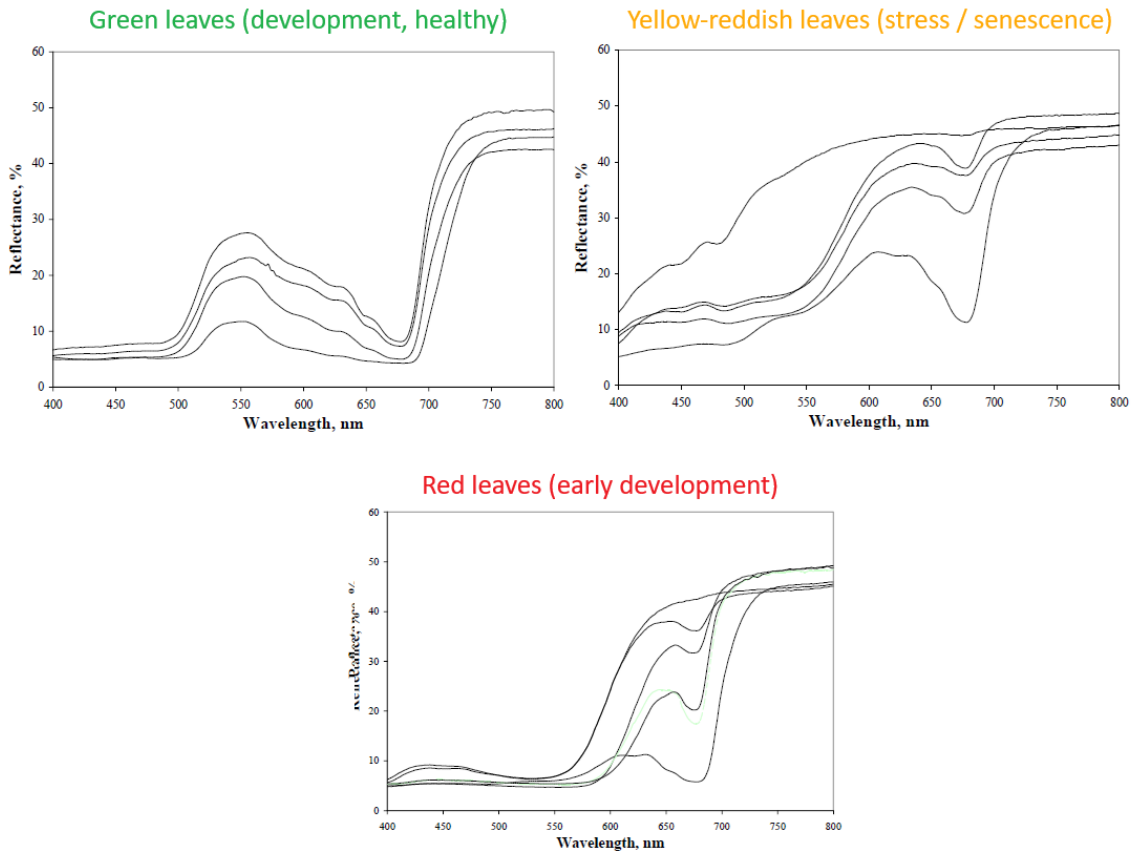

Figure 5: Spectral signatures of leaves at different phenological stages and stress conditions. Top left: Green (healthy) leaves showing characteristic chlorophyll absorption in blue and red regions with prominent green peak and near-infrared plateau. Top right: Yellow-reddish leaves representing early senescence or stress conditions with elevated visible reflectance and reduced red absorption. Bottom: Red leaves indicating advanced senescence with strong anthocyanin absorption in green-yellow region, minimal chlorophyll absorption, and complete loss of red edge feature. Colored bullet points indicate developmental stage: red (beginning of vegetation), green (healthy development), and yellow-orange (stress/senescence).

Multiple curves represent natural variability within healthy vegetation—different species, leaf ages, or environmental conditions—but all share the fundamental pattern of strong chlorophyll absorption bracketing the green reflectance peak. This signature corresponds to the "Development (healthy)" stage marked in green on the figure, representing peak photosynthetic activity and optimal physiological function (Peñuelas, Filella, Biel, Serrano, and Save 1993).

5.2 Yellow-Reddish Leaves: Stress and Senescence

The yellow-reddish leaf spectra (top right, Figure 5) show systematic departures from the healthy baseline:

- **Elevated reflectance** across the entire visible spectrum (400-700 nm) as chlorophyll degrades
- **Broadened and increased green-yellow reflectance** (500-600 nm) revealing underlying carotenoids
- **Reduced red absorption depth** as chlorophyll concentration declines
- **Gentler red edge slope** indicating lower chlorophyll content
- **Slightly reduced near-infrared reflectance** in some cases, suggesting changes in leaf internal structure

These spectral changes correspond to **stress or senescence conditions** (marked in yellow-orange bullets on the figure) where chlorophyll synthesis is impaired or degradation accelerated (Carter 1993). During stress or senescence, chlorophyll degrades while carotenoids persist longer, creating the characteristic yellow-orange appearance.

5.3 Red Leaves: Beginning of Vegetation

The red leaf spectra (bottom, Figure 5) represent young, developing leaves at the beginning of the growing season:

- **Elevated visible reflectance** (400-700 nm) due to lower chlorophyll content in developing leaves
- **Strong absorption** in green-yellow region (520-600 nm) from anthocyanin accumulation
- **Moderate red absorption** as chlorophyll is still developing
- **Less pronounced red edge** compared to mature leaves due to lower chlorophyll content
- **Lower near-infrared reflectance** than mature leaves, reflecting developing leaf structure

This spectral signature, marked as "Beginning of vegetation" with red bullets in the figure, indicates early spring leaf development where anthocyanins accumulate for photoprotection while the photosynthetic apparatus is still maturing (Chalker-Scott 1999). Young leaves often produce anthocyanins to protect developing chloroplasts from photo-oxidative damage

during the vulnerable expansion phase. As leaves mature and the photosynthetic machinery becomes fully functional, anthocyanin content typically decreases and chlorophyll dominates, transitioning to the green leaf signature.

5.4 The Phenological Continuum

The progression from red (early development) through green (mature, healthy) to yellow-reddish (stress/senescence) leaves represents different physiological states that can be monitored remotely (Gitelson, Merzlyak, and Chivkunova 2001). Importantly, this highlights a challenge in remote sensing: both young developing leaves and senescing leaves can show elevated anthocyanin content, but for different physiological reasons. Distinguishing between these states requires temporal context—spring observations of red spectra likely indicate new growth, while autumn observations suggest senescence. Vegetation indices designed to capture these transitions must account for the changing relationships between pigments and the multiple roles of anthocyanins across the growing season (Richardson et al. 2018).

6 Structural Components: Beyond Pigments

While pigments dominate the visible spectrum, structural and biochemical components beyond pigments create diagnostic features in the near-infrared and shortwave infrared regions (Curran 1989). Figure 6 focuses on epicuticular waxes, protective coatings on leaf surfaces that serve multiple functions including water regulation, pathogen defense, and UV protection (Shepherd and Nichols 2006). Similarly to chlorophyll, wax concentration is highest at the peak of the vegetation season.

The electron microscopy images in Figure 6 show dramatic differences in leaf surface structure before and after wax removal, revealing the crystalline wax structures that coat healthy leaf surfaces. The spectral consequences of wax removal are striking:

- **Before removal** (top curve): Highest reflectance across the entire spectrum, particularly in the near-infrared (750-1700 nm) where wax creates a highly reflective surface
- **After 10 seconds of removal**: Intermediate reflectance as surface wax is partially dissolved
- **After 30 seconds of removal** (bottom curve): Lowest reflectance as most surface wax has been eliminated

Notably, the wax removal experiment demonstrates the phenomenon of **blue shift**, where the reflectance spectrum shifts systematically toward shorter wavelengths as wax is removed (**grant1987diffuse?**). This blue shift occurs because epicuticular waxes preferentially scatter longer wavelengths; their removal reduces this scattering effect, causing the spectral curves to shift toward the blue end of the spectrum. This phenomenon has important implications for

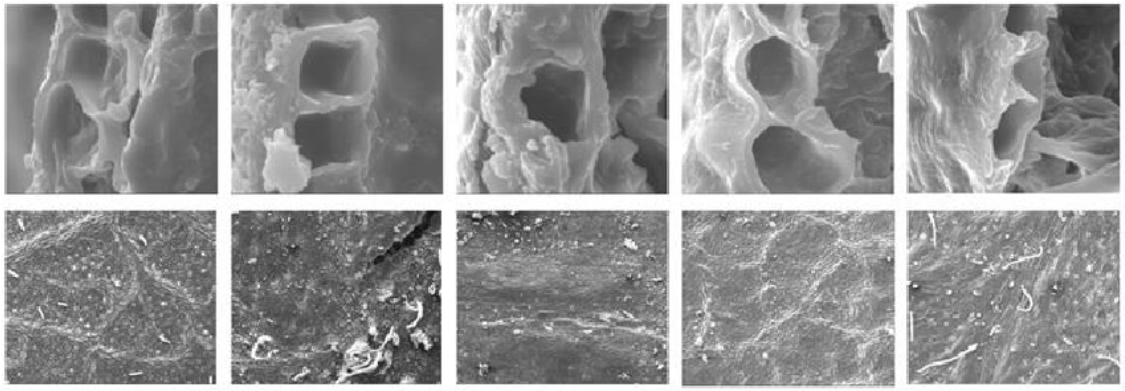

a

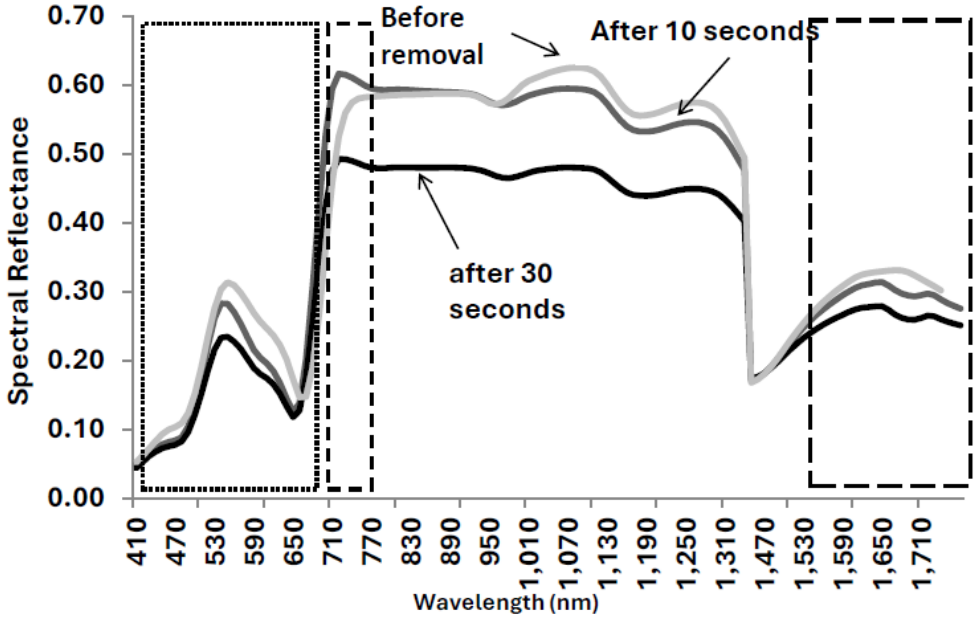

b

Figure 6: Impact of epicuticular wax on leaf spectral reflectance. a: Scanning electron microscopy (SEM) images showing leaf surface microstructure with intact epicuticular wax crystals (top row) and after wax removal (bottom row) at different times. b: Spectral reflectance curves (410-1710 nm) demonstrating the effect of wax removal on reflectance across visible, near-infrared, and shortwave infrared regions. Three curves show reflectance before wax removal (highest), after 10 seconds of removal (intermediate), and after 30 seconds of removal (lowest), with the greatest differences observed in the near-infrared region (750-1250 nm).

interpreting spectral changes in vegetation experiencing drought stress or other conditions that affect wax production or integrity.

The spectral regions most sensitive to wax content are:

- **Blue-green** (410-550 nm): Moderate sensitivity with elevated reflectance in waxy leaves
- **Near-infrared** (750-1250 nm): High sensitivity throughout this region
- **Shortwave infrared** (1300-1700 nm): Continued sensitivity to wax content

The practical implication is that vegetation indices targeting wax content must operate in spectral regions where wax effects dominate over pigment absorption. The reciprocal of the square root of reflectance differences in specific wavelength regions provides a measure of wax content:

$$\frac{1}{\sqrt{R_{750-770} - R_{490-500} - R_{660-690}}}$$

Beyond waxes, other structural components create diagnostic spectral features:

- **Cellulose and lignin**: Absorption bands in the shortwave infrared around 2100 nm (Curran 1989)
- **Leaf water content**: Strong absorption features at 970 nm, 1200 nm, 1450 nm, and 1940 nm (Peñuelas, Filella, Biel, Serrano, and Savé 1993)
- **Leaf internal structure**: Determines the overall magnitude of near-infrared reflectance through multiple scattering (Jacquemoud and Baret 1990)

These structural and compositional properties interact with pigment signals, creating the full complexity of vegetation spectra that extends from 400 nm through 2500 nm in comprehensive hyperspectral datasets (Ustin and Gamon 2009).

7 From Spectral Signatures to Quantitative Estimation

The theoretical framework presented here—linking specific biochemical compounds to characteristic spectral features—forms the foundation for quantitative remote sensing of vegetation functional traits (Homolová et al. 2013). The key principles that enable this translation from photons to plant physiology are:

1. **Spectral specificity**: Each compound has characteristic absorption features at particular wavelengths, enabling selective detection (Gates et al. 1965)
2. **Concentration dependence**: Reflectance changes systematically with biochemical concentration, allowing quantitative estimation (Jacquemoud and Baret 1990)
3. **Temporal dynamics**: Seasonal patterns in biochemistry create predictable spectral trajectories (Richardson et al. 2018)

4. **Structural modulation**: Leaf and canopy architecture affect spectral signals independently of biochemistry, requiring normalization strategies (Asner 1998)

The practical implementation of these principles through vegetation indices and statistical models—demonstrated in the following tutorial sections—provides operational tools for extracting biological information from hyperspectral data (Verrelst et al. 2015). By understanding the physical and physiological basis of these spectral-biochemical relationships, researchers can develop robust methods for monitoring plant functional traits across scales, from controlled laboratory measurements to satellite-based global vegetation monitoring (Ustin and Gamon 2009).

This theoretical foundation prepares you to interpret the analytical methods demonstrated in the practical tutorial that follows, where we transform raw spectral measurements into quantitative estimates of plant functional traits through statistical analysis and machine learning classification.

8 References

Asner, Gregory P. 1998. "Biophysical and Biochemical Sources of Variability in Canopy Reflectance." *Remote Sensing of Environment* 64 (3): 234–53.

Asner, Gregory P, and Roberta E Martin. 2015. "Quantifying Forest Canopy Traits: Imaging Spectroscopy Versus Field Survey." *Remote Sensing of Environment* 158: 15–27.

Carter, Gregory A. 1993. "Responses of Leaf Spectral Reflectance to Plant Stress." *American Journal of Botany* 81 (2): 239–43.

Chalker-Scott, Linda. 1999. "Natural Antioxidants from Plant Material in Photosensitive Disorders." *Photochemistry and Photobiology* 70 (1): 1–9.

Curran, Paul J. 1989. "Remote Sensing of Foliar Chemistry." *Remote Sensing of Environment* 30 (3): 271–78.

Demmig-Adams, Barbara, and William W Adams III. 2006. "Photoprotection in an Ecological Context: The Remarkable Complexity of Thermal Energy Dissipation." *New Phytologist* 172 (1): 11–21.

Gates, David M, Harry J Keegan, John C Schleter, and Victor R Weidner. 1965. "Spectral Properties of Plants." *Applied Optics* 4 (1): 11–20.

Gitelson, Anatoly A, Yuri Gritz, and Mark N Merzlyak. 2003. "Relationships Between Leaf Chlorophyll Content and Spectral Reflectance and Algorithms for Non-Destructive Chlorophyll Assessment in Higher Plant Leaves." *Journal of Plant Physiology* 160 (3): 271–82.

Gitelson, Anatoly A, Yoram J Kaufman, Robert Stark, and Don Rundquist. 2002. "Novel Algorithms for Remote Estimation of Vegetation Fraction." *Remote Sensing of Environment* 80 (1): 76–87.

Gitelson, Anatoly A, Galina P Keydan, and Mark N Merzlyak. 2006a. "Remote Estimation of Chlorophyll Content in Higher Plant Leaves." *International Journal of Remote Sensing* 27 (12): 2055–66.

———. 2006b. "Three-Band Model for Noninvasive Estimation of Chlorophyll, Carotenoids, and Anthocyanin Contents in Higher Plant Leaves." *Geophysical Research Letters* 33 (11).

Gitelson, Anatoly A, Mark N Merzlyak, and Olga B Chivkunova. 1999. "Non-Destructive Optical Detection of Pigment Changes During Leaf Senescence and Fruit Ripening." *Physiologia Plantarum* 106 (1): 135–41.

———. 2001. "Non-Destructive Assessment of Chlorophyll Carotenoid and Anthocyanin Content in Higher Plant Leaves: Principles and Algorithms." *Remote Sensing for Agriculture and the Environment* 1: 78–94.

Gitelson, Anatoly A, Andrés Viña, Verónica Ciganda, Donald C Rundquist, and Timothy J Arkebauer. 2006. "Signature Analysis of Leaf Reflectance Spectra: Algorithm Development for Remote Sensing of Chlorophyll." *Journal of Plant Physiology* 163 (3): 1176–85.

Gould, Kevin S. 2004. "Nature's Swiss Army Knife: The Diverse Protective Roles of Anthocyanins in Leaves." *Journal of Biomedicine and Biotechnology* 2004 (5): 314–20.

Hesketh, Michael, and Arturo Sánchez-Azofeifa. 2020. "Seasonal and Interannual Spectral Variability of Plant Functional Types in a Northern Mixed Grassland." *Remote Sensing* 12 (5): 674.

Hoch, William A, Erika L Zeldin, and Brent H McCown. 2001. "Physiological Significance of Anthocyanins During Autumnal Leaf Senescence." *Tree Physiology* 21 (1): 1–8.

Homolová, Lucie, Zbyněk Malenovský, JGPW Clevers, Glenda García-Santos, and Michael E Schaepman. 2013. "Review of Optical-Based Remote Sensing for Plant Trait Mapping." *Ecological Complexity* 15: 1–16.

Horler, DNH, M Dockray, and J Barber. 1983. "The Red Edge of Plant Leaf Reflectance." *International Journal of Remote Sensing* 4 (2): 273–88.

Huete, Alfredo, Kamel Didan, Tomoaki Miura, E Patricia Rodriguez, Xiang Gao, and Laerte G Ferreira. 2002. "Overview of the Radiometric and Biophysical Performance of the MODIS Vegetation Indices." *Remote Sensing of Environment* 83 (1-2): 195–213.

Jacquemoud, Stéphane, and Frédéric Baret. 1990. "PROSPECT: A Model of Leaf Optical Properties Spectra." *Remote Sensing of Environment* 34 (2): 75–91.

Lichtenthaler, Hartmut K. 1987. "Chlorophylls and Carotenoids: Pigments of Photosynthetic Biomembranes." *Methods in Enzymology* 148: 350–82.

Peñuelas, Josep, Iolanda Filella, Corina Biel, Lluis Serrano, and Robert Save. 1993. "The Reflectance at the 950–970 Nm Region as an Indicator of Plant Water Status." *International Journal of Remote Sensing* 14 (10): 1887–1905.

Peñuelas, Josep, Iolanda Filella, Corina Biel, Lluis Serrano, and Robert Savé. 1993. "The Reflectance at the 950–970 Nm Region as an Indicator of Plant Water Status." *International Journal of Remote Sensing* 14 (10): 1887–1905.

Richardson, Andrew D, Mariah S Carbone, Trevor F Keenan, Claudia I Czimczik, David Y

Hollinger, Patty Murakami, Paul G Schaberg, and Xiaomei Xu. 2013. "Seasonal Dynamics and Age of Stemwood Nonstructural Carbohydrates in Temperate Forest Trees." *New Phytologist* 197 (3): 850–61.

Richardson, Andrew D, Trevor F Keenan, Mirco Migliavacca, Youngryel Ryu, Oliver Sonnentag, and Michael Toomey. 2018. "Tracking Vegetation Phenology Across Diverse North American Biomes Using PhenoCam Imagery." *Scientific Data* 5 (1): 1–24.

Shepherd, KA, and JP Nichols. 2006. "The Measurement of Plant Diversity in the Mid-Visible and Near-Infrared." *Remote Sensing of Environment* 100 (3): 384–97.

Ustin, Susan L, and John A Gamon. 2009. "Remote Sensing of Plant Functional Types." *New Phytologist* 186 (4): 795–816.

Verrelst, J, Z Malenovský, C Van der Tol, G Camps-Valls, JP Gastellu-Etchegorry, P Lewis, P North, and J Moreno. 2015. "Optical Remote Sensing and the Retrieval of Terrestrial Vegetation Bio-Geophysical Properties–a Review." *ISPRS Journal of Photogrammetry and Remote Sensing* 108: 273–90.